Roso, VR.; Santos, NDSA.; Valle, RM.; Castilla Alvarez, CE.; Monsalve-Serrano, J.; García Martínez, A. (2019). Evaluation of a stratified prechamber ignition concept for vehicular applications in real world and standardized driving cycles. Applied Energy. 254:1-13. https://doi.org/10.1016/j.apenergy.2019.113691

# Evaluation of a stratified prechamber ignition concept for vehicular applications in real world and standardized driving cycles

**Vinícius Rückert Roso[a], Nathália Duarte Souza Alvarenga Santos[a], Ramon Molina Valle[a], Carlos Eduardo Castilla Alvarez[b], Javier Monsalve-Serrano[c], Antonio García[c]**

**[a] CTM – Centro de Tecnologia da Mobilidade, Universidade Federal de Minas Gerais, Belo Horizonte, MG, Brazil**

**[b] Departamento de Engenharia Mecânica, Universidade Federal de Lavras**

**[c] CMT – Motores Térmicos, Universitat Politècnica de València, Camino de Vera s/n, 46022 Valencia, Spain**

*Applied Energy, Volume 254, 15 Nov 2019, 113691*

https://doi.org/10.1016/j.apenergy.2019.113691

**Abstract**

The aim of this paper is to evaluate the potential of a prechamber ignition system to reduce the exhaust emissions and fuel consumption of commercial vehicles in the conditions proposed by the standardized and real-world driving cycles. For this purpose, a multi-cylinder engine was mapped in stationary conditions using two different combustion modes. First, the engine was tested under the baseline stoichiometric combustion with a spark plug ignition system. Second, the engine map was obtained using a stratified prechamber ignition system under lean conditions. Later, the experimental data was used as input for a computer model that simulates the vehicle operation with both concepts under different driving cycles. To run the model under real-world driving conditions, experimental data was acquired in a specific region in southern Brazil in conditions of heavy and free flow. Moreover, the conditions of the study were extended including two homologation cycles, the FTP-75 and WLTC. The results for the different cycles show similar average exhaust emissions and fuel consumption between WLTC and the real conditions of free flow traffic, and also between the FTP-75 and the real conditions of heavy flow traffic. The results also point out the potential of the prechamber ignition system to achieve a reduction of the engine-out CO and $NO_x$ emissions greater than 50% and 85%, respectively, as compared to the baseline stoichiometric combustion with a spark plug ignition, without penalizing the fuel consumption.

**Keywords**
Pre-chamber; driving cycle; vehicular application; lean combustion.

## 1. Introduction

Aiming at the improvement of air quality, vehicular emission regulations were already introduced in California and Japan in the 60's and in Europe in the 70's [1], presenting increasingly restrictions to the current Euro VI [2] and Proconve P-7 [3], for example. According to the International Panel of Climate Changes (IPCC), the emission regulations had positive results as since they were implemented, the emissions from the transportation sector presented lower increase than the vehicular fleet [4]. This result has been reached because the vehicular manufacturers adopted technologies, fuels and strategies to reduce and control the regulated emissions, aiming to target the imposed values.

The use of fuels produced from renewable sources has been encouraged by both the scarcity of fossil fuels and their potential in reducing gaseous emissions [5]. In terms of emissions, it is justified because the amount of $CO_2$ released due to fuel combustion is compensated by the

regrowth of the plants used in fuel production, which will absorb a similar amount of $CO_2$ during photosynthesis, making ethanol as $CO_2$ free. Besides that, Brazilian commercial ethanol also presents lower percentages of hydrocarbon in volumetric composition if compared to fossil fuels, being able to reduce the HC emissions. Furthermore, some ethanol properties such as the higher octane number, the latent heat of vaporization and the fast laminar speed, made ethanol one of the most promising biofuels [6]. These characteristics help to mitigate knock in SI engine, allowing the use of higher volumetric compression ratio and, consequently, improving the engine global efficiency [7]. In this sense, the use of biofuels as ethanol combined with new technologies for internal combustion engines seems as an interesting alternative [8, 9]. Added to it, dual-fuel strategies [10, 11] and the use of fuels with fast flame speed [12] has also been highlighted and extensively studied, presenting positive results for combustion and engine-out emissions.

At the beginning of vehicular emission regulations, an approach that presented good results on increasing engine efficiency and reducing exhaust emissions was the lean burn concept. The lower average temperatures of lean combustion decreases heat losses to the cylinder walls [13] and also reduces the formation of undesired pollutant emissions such as $NO_x$, which are more prone to be developed under high temperatures [14]. Also, since SI engines are particularly sensitive to the air-fuel ratio, combustion can be more complete with a small excess of air, reducing the production of CO and HC, typical compounds of incomplete combustion [15].

Despite the benefits of lean combustion, lower burn velocities result in higher cyclic variability, requiring a greater source of energy to ignite the mixture [16]. Among other technologies used to improve the amount of ignition energy, the use of prechamber ignition system (PCIS) is already well stablished for lean combustion [17-19] and has already been used by the automotive industry for commercial applications [20-25]. However, only few studies have published results of PCIS in vehicular conditions. Date et al. [20] pointed to expressive reduction in CO, HC and $NO_x$ emissions for three different engines with PCIS if compared to the original ones when covering transient cycles of federal standards. Added to this, Attard et al. [26] observed more than 6% of fuel economy during NEDC (New European Driving Cycle) and FTP-75 (Federal Test Procedure) simulation when using a PCIS.

Even with the positive effects of emission regulations, the standard driving cycles present limitations because they were developed using specific and restrict routes, reducing their representativeness when compared to real situations. In this sense, some studies, especially in Europe, have also pointed out the significant differences observed between the emissions observed in standardized tests and in real driving conditions [27, 28]. This fact has direct impacts on environmental protection policies, since the most national air emission inventories are compiled by means of computerised emission models and results from type approval test results [29-31]. These divergences have had even more emphasis after the episode known as “Volkswagen fraud”, in which the vehicles were programmed to fulfil the legislative requirements under the well-controlled conditions of the test cycle in chassis dynamometer, but had totally different behaviour when in real-world conditions [32]. Thus, due to their low coverage and liability to fraud, since 2017 European countries have been using more inclusive procedures encompassing currently developed cycles and real driving emission compensations [33].

Experimental [34, 35] and computational methods are widely observed in literature to estimate vehicular emissions and fuel consumption under driving conditions. Among them, transient predictions based on experimental data from stationary points has been used to investigate combustion strategies [36], hybrid concepts [37, 38], fuel combinations [39] and aftertreatment systems [40] when in vehicular application over driving cycles, optimizing the development of systems and strategies.

With this, at least two approaches carried out in this research are innovative, one related to the driving cycles and the other to the proposed ignition system. No comparison between Brazilian real-world emission rates and the certification standards is reported in the literature, even as is uncommon the evaluation of PCIS in all of the engine map ranges. With the concern on vehicular emissions under real conditions, this paper aims to evaluate exhaust emissions and fuel consumption of a passenger car using a PCIS, over real and standard driving cycles. For this, transient behaviour in different driving cycles will be compared through simulations that were carried out using dedicated vehicle models and steady-state experimental maps of emissions and performance. This experimental and simulation procedure present an effective methodology for the evaluation of system behaviour before the implementation in vehicles, enabling the optimization of gear shifting strategy and the resultant engine-out emissions and fuel consumption.

## 2. Methodology

The methodology used to tackle the objectives of the study combines experimental and numerical tools. This section describes the experimental facility used to acquire the engine data as well as the computational models developed to simulate the vehicle behaviour operating with both combustion concepts. Moreover, the methodology followed to acquire the real driving profiles used as inputs for the model is described.

### 2.1. Engine experimental setup

The experimental tests were performed using a commercial spark ignition (SI) engine, whose main characteristics are described in Table 1. The initial tests were developed with the baseline engine, calibrated for stoichiometric conditions, and using Brazilian ethanol as fuel. In a second step, the experimental tests were performed substituting the conventional spark plug ignition system by a prechamber ignition system (PCIS) [41, 42], without other mechanical changes. This system is composed of a prechamber and a main combustion chamber. The prechamber has an internal volume of 0.88 $cm^3$, representing 2.2% of the main combustion chamber volume. The prechamber has five interconnecting holes to the main combustion chamber, four of which have 1 mm of diameter and an angle of 45° versus the normal axe, and the remaining one is located at the centre of the prechamber end, with a diameter of 2 mm.

The prechamber ignition system uses two different fuels. Brazilian commercial ethanol (E96) is injected into the main combustion chamber, where E96 denotes hydrous ethanol with ethanol volumetric percentage between 95.1% and 96% [43, 44]. The E96 characteristics are presented in Table 2 [45]. In a previous research, this biofuel presented combustion and emission benefits over the gasoline, especially when operating with lean mixtures [46]. On the other hand, the prechamber is fed with hydrogen fuel at 10 bar injection with a LHV of 120.0 MJ/kg. This leads to a mixture stratification between the prechamber and the main combustion chamber. By this reason, this prechamber ignition system is so-called active [19] or of stratified charge [17].

Table 1. Engine technical specification.

| Characteristics | |
|---|---|
| Displacement Volume | 1596 cm³ |
| Number of Cylinders | 4 |
| Main chamber injection type | Port-fuel injection |
| Prechamber injection type | Direct injection |
| Ignition system | Spark plug / Prechamber |
| Connecting-rod length | 137 mm |
| Bore x stroke | 79.0 x 81.4 mm |
| Geometric compression ratio | 11.0:1 |
| Intake valve opening (B-TDC) | 10° (1 mm ref.) |
| Intake valve closure (A-BDC) | 20° (1 mm ref.) |
| Exhaust valve opening (B-BDC) | 30° (1 mm ref.) |
| Exhaust valve closure (A-TDC) | 0° (1 mm ref.) |
| Fire order | 1-3-4-2 |

Table 2. Specification of Brazilian commercial ethanol.

| Property | |
|---|---|
| Density (kg/m³) | 808.7 |
| Carbon (%m/m) | 50.7 |
| Hydrogen (%m/m) | 13.0 |
| Oxygen (%m/m) | 36.3 |
| Molar ratio (H/C) | 3.0 |
| Ethanol (%v/v) | 95.7 |
| Water (%v/v) | 4.3 |
| Stoichiometry | 8.8 |
| LHV (MJ/kg) | 24.76 |

The engine was instrumented with the data acquisition systems shown in Figure 1, which can be divided into five subgroups. The first one is the engine management system, executed through a MoTeC M800 device. The second one is a MoTeC M400 device used to control the hydrogen injection. The third acquisition system is the IndiModul X Tension used to acquire the pressure cylinder data used for the combustion analysis. The forth system is the Stars, from Horiba, used to control the dynamometer and acquire the test data. The last one is the OBS-2200 measurement system, from Horiba, used to collect exhaust gas samples and analyse it regarding its emission concentration. The OBS system uses a non-dispersive infrared (NDIR) analyser to measure CO and $CO_2$, a flame ionization detector (FID) analyser to measure THC, a chemiluminescent detection (CLD) analyser to measure nitrogen compounds. The measurement of exhaust emissions in these tests considered raw gases, without any aftertreatment. This is because no aftertreatment models are used in the simulations.

To control the engine load in the tests, a Horiba - TITAN S470 Foucault passive dynamometer was used. This dynamometer is installed in a dynamic room that allows the control of the temperature of the cooling water of the engine, oil temperature and ethanol injection pressure, fixed for all the tests at 90 °C, 100 °C and 3 bar, respectively.

The in-cylinder pressure was measured by the electric pressure transducer GH14P, from AVL. The electric signal coming from this transducer passes through the amplifier Micro IFEM, also from AVL, to its conditioning and amplification. For measurements of absolute pressure, the sensor LP11DA from AVL was installed at the intake manifold. A piezo resistive sensor LP21DA, also from AVL, measured pressure at exhaust manifold. An optical encoder producing digital signal was installed to indicate the crankshaft angle. The angle measurements, along with the pressure recordings provide pressure data in 0.1° of crankshaft breaks. The accuracy of the different devices used to acquire data is summarized in Table 3.

To ensure the reliability of the combustion parameters acquired, their values were averaged from a substantial number of individual cycle analysis results. Combustion parameters obtained from the software Indicom are an average of 200 combustion cycles. The ECU data recorded by the MoTeC devices were collected at an average of 30 seconds in a frequency of 50 Hz. Dynamometer data from Stars system were acquired in 20 seconds in a frequency of 10 Hz and exhaust data from OBS were acquired during 60 seconds with the frequency of 1 Hz.

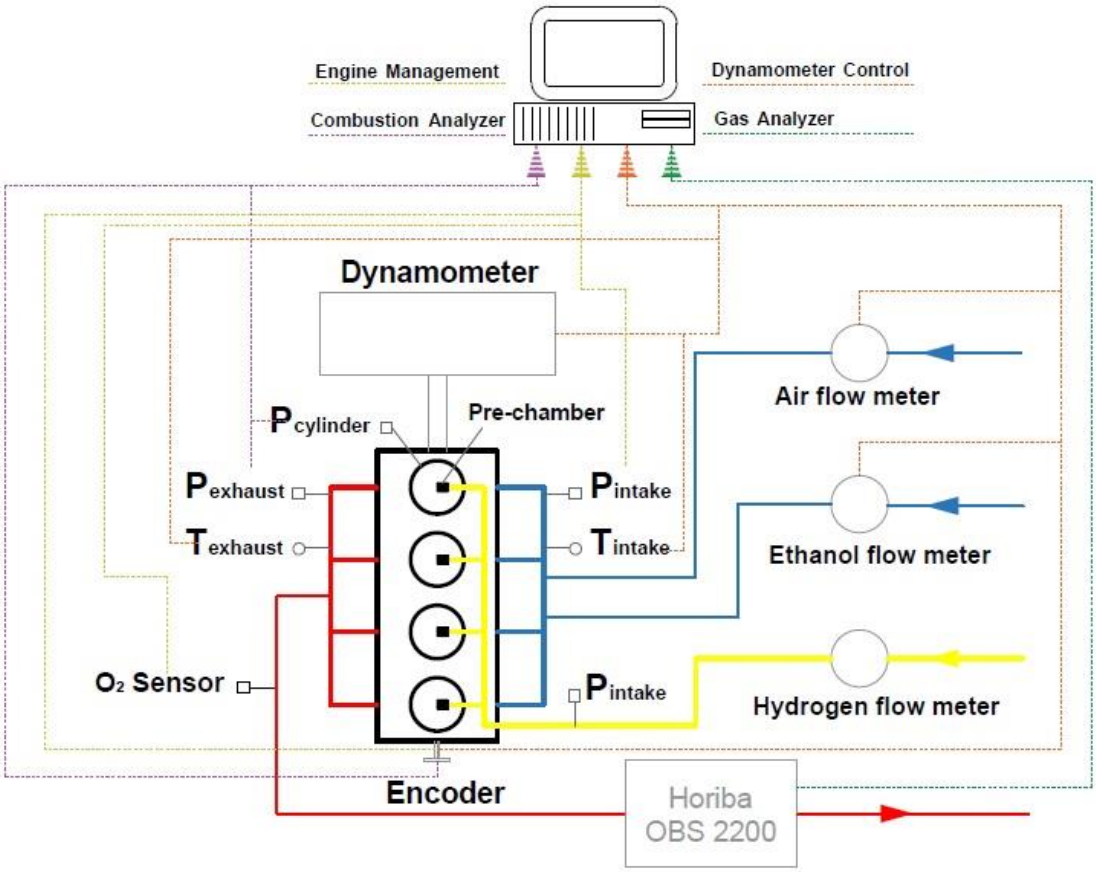


Figure 1. Schematic diagram of engine instrumentation assembling.

Table 3. Accuracy of the instrumentation used in the engine experimental work.

| Variable measured | Device | Manufacturer/model | Accuracy |
|---|---|---|---|
| In-cylinder pressure | Piezoelectric | AVL/GH14P | ± 0.3 ES |
| Intake pressure | Piezo resistive | AVL/LP11DA | ± 0.1% ES |
| Exhaust pressure | Piezo resistive | AVL/LP21DA | ± 0.1% ES |
| Water temperature | Thermo resistive | PT100 | ± 0.1% ES |
| Oil temperature | Thermocouple | TC direct/type K | ± 0.4% ES |
| Exhaust temperature | Thermocouple | TC direct/type K | ± 0.4% ES |
| Intake temperature | Thermocouple | TC direct/type K | ± 0.4% ES |
| Crank angle and engine speed | Encoder | AVL/365C AngleEncoder | <± 0.03° |
| $NO_x$, CO, HC, $CO_2$ | Gas analyzer | Horiba/OBS2200 | ± 1% |
| Ethanol mass flow | Coriolis flow meter | Metroval/Rheonik RHE 08 | ± 0.2% MV |
| Air mass flow | Air flow meter | ABB/Sensyflow P (FMT700-P) | ± 3% MV |
| Engine load | Load cell | HBM/Class DI TC 5022 | <± 0.2% ES |

An interactive strategy between the injection timing, injection duration and ignition timing parameters was performed to achieve an optimized condition during the engine calibration. The injection timing was calibrated to achieve the lowest coefficient of variation of IMEP ($CoV_{IMEP}$), acceptable until 5% [47]. The injection duration was adjusted to maintain the desired global lambda and the spark advance to obtain the maximum brake torque without knocking. Any change in one of these three parameters interferes in the others, being an interactive process. Regarding the PCIS, the injection of hydrogen was increased until achieving the lowest possible $CoV_{IMEP}$, being the fuel burned in prechamber a mixture of ethanol from the main chamber and hydrogen injected in prechamber.

Figure 2 shows the experimental operating points evaluated in steady-state conditions with the baseline ignition system and with the PCIS. The tested operating range was the same for both systems, with the engine speed range varying from 1500 rpm to 3000 rpm in steps of 250 rpm, and five different accelerator positions from 0% to 100%. Engine speeds above those, as idle condition, 1000 rpm and 1250 rpm, where evaluated under less load points because they occur only at start or stop times. Hence, different regions of the map are covered, ranging from idle conditions to medium and high loads, encompassing urban and road driving situations. The experimental points for the baseline ($\lambda$=1.0) and for the PCIS ($\lambda$=1.4) were substantially different due to the lower amount of fuel in the lean burn (Figure 2). By this reduction of IMEP in wide open throttle (WOT) conditions, it was necessary to redivide the five accelerator position points.

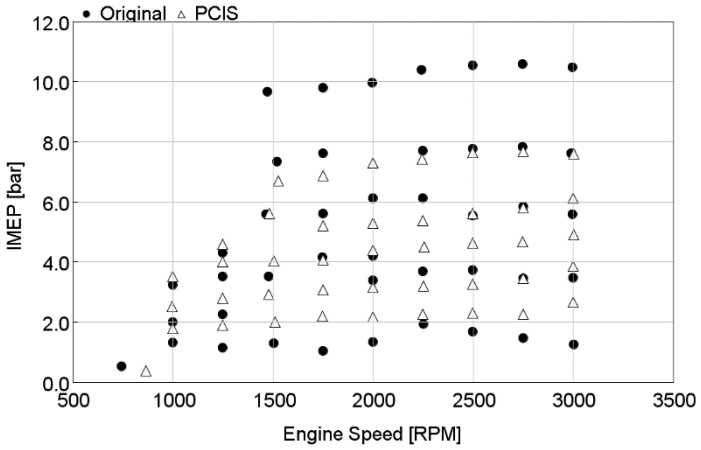


Figure 2. Experimental steady-state operation points for both ignition systems.

### 2.2. Driving cycles

A representative route of the urban buses in Santa Maria city, southern Brazil, was considered to evaluate the real driving conditions [48, 49]. The driving cycle under investigation consists of a mixed route, comprising urban and highway portions, over a total of 11.7 km. Figure 3 shows the route over the city map and the altitude profile, consisting of 179 and 151 meters of altitude gain and loss respectively, and a difference of 28 meters between the initial and final altitude. Two real traffic conditions were evaluated, one considering free flow, and other with heavy flow. An On-Board-Diagnostic (OBD) OBD-II system was used to acquire the data at a rate of 20 Hz to be processed for the driving cycle formulation.

Apart from the real driving cycles in different traffic conditions, an analysis of a Brazilian test procedure will be performed by considering the FTP-75 type approval cycle in the study. The emissions and performance analysis of the system application will be also conducted over the Worldwide harmonized Light vehicles Test Cycles (WLTC), considered in UNECE Global technical regulation No 15 (GTR 15) [50]. The standard and real cycles are presented in Figure 4 (a) and (b), respectively.

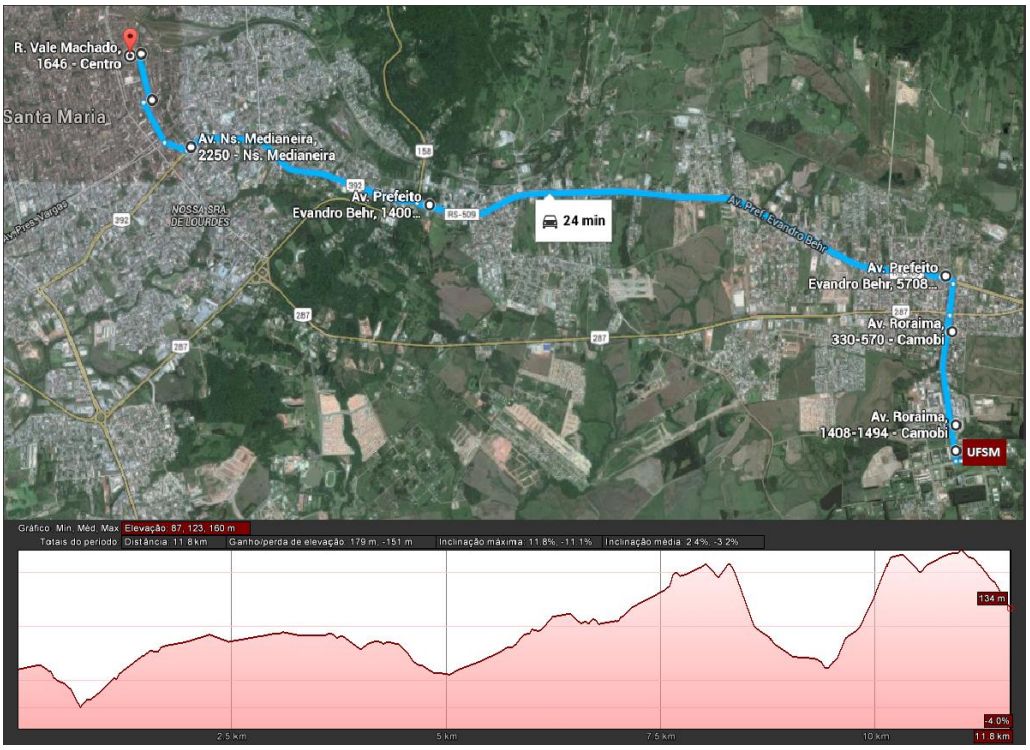


Figure 3. Route of 11.7km in southern Brazil considered for real driving analysis [48].

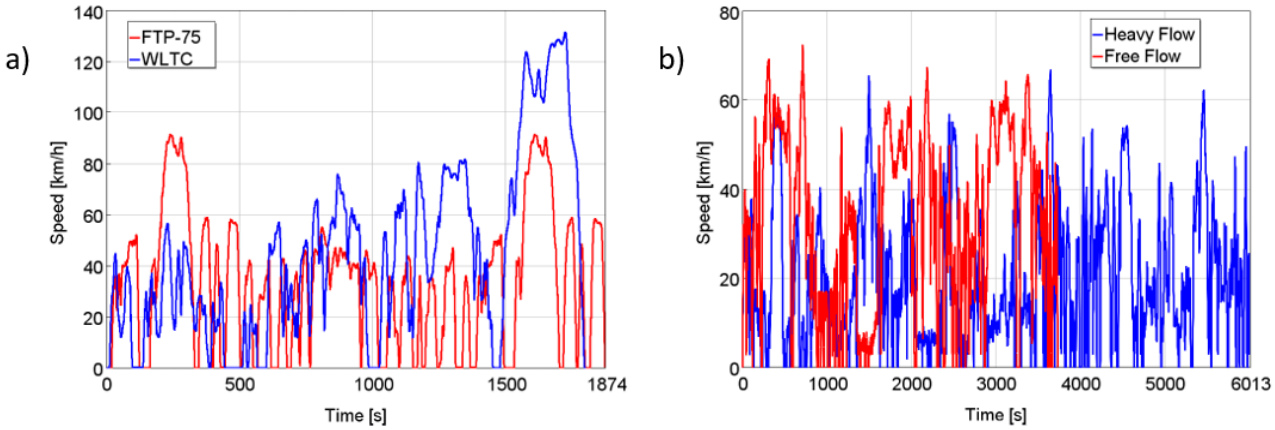


Figure 4. Standard (a) and real (b) driving cycles considered for the passenger car simulation.

Standard cycles are usually evaluated using the *Art.Kinema* utility that creates three output files, one of which includes the smoothed speed profile and the values of the kinematic parameters [51]. Table 4 presents these characteristics for the considered driving cycles, with parameters for real conditions being calculated through the equations observed in literature [52]. Real-world cycles operate at lower average speeds because of the traffic conditions, presenting much higher acceleration rates. These lower speeds also subsequently mean that vehicle operates at lower gear ratios with higher engine speeds. Dispersion in negative values indicates intensive braking by the vehicle, whereas in standard cycles, acceleration and deceleration are almost equal. In this sense, average positive acceleration indicates the degree of overall positive acceleration in a driving pattern. Higher acceleration implies higher energy demands, thus higher emissions and fuel consumption. Root Mean Square (RMS) acceleration is a measure of how frequently and how much acceleration varies over the driving cycle, with high values indicating rapid acceleration and breaking [53], being the most expressive characteristic of real conditions. Positive Kinetic Energy (PKE) is the acceleration energy required in a certain driving

pattern and can be used to indicate how much energy the engine needs to produce to follow a certain driving pattern, being one of the best indicators for engine emission prediction [54]. Relative Positive Acceleration (RPA) is a value that characterizes the load of the trip and it is used as a factor to compare different test cycles [55]. All of these parameters presented in Table 4, from which it can be inferred a greater aggressiveness during the real driving cycles. This will have a direct impact on fuel consumption and exhaust emissions.

Table 4. Comparison between driving cycles characteristics.

| | **Standard Cycles** | | **Real Cycles** | |
|---|---|---|---|---|
| | **FTP-75** | **WLTC** | **Free Flow** | **Heavy Flow** |
| Duration time [s] | 1874.00 | 1800.00 | 3738.17 | 6013.09 |
| Distance [km] | 17.77 | 23.20 | 35.40 | 35.40 |
| Average Speed [m/s] | 11.65 | 12.92 | 9.38 | 5.84 |
| Average positive acceleration [m/s²] | 0.22 | 0.18 | 0.55 | 0.43 |
| Average negative acceleration [m/s²] | -0.21 | -0.18 | -0.50 | -0.46 |
| RMS acceleration [m/s²] | 0.63 | 0.53 | 2.83 | 2.49 |
| PKE [m/s²] | 0.35 | 0.31 | 0.42 | 0.42 |
| RPA [m/s²] | 0.16 | 0.16 | 0.22 | 0.22 |

### 2.3. Modelling procedure

The first of the two models considers a car operating in stoichiometric conditions using a conventional spark plug ignition system. The second model considers the same commercial vehicle, but using a stratified prechamber ignition system operating with a global lambda factor of 1.4. Both models use steady-state experimental maps of emissions and performance as input data.

In order to evaluate the ignition system effects on emissions and performance when applied to a passenger car under real and standard conditions, different driving cycles were considered in two zero-dimensional computer model, developed with GT-Suite software from Gamma Technologies®. Figure 5 shows the logical representation of the model, connecting the various components of the system and their sub-models. Constructive and mechanical data as transmission ratios, vehicle mass and aerodynamic coefficients were inputted in the *vehicle* unit. In the *driver* unit were added driving parameters as the driving cycle, gear shift strategy, accelerator and brake positions. In the sub-model *engine* are the engine maps of performance, fuel consumption and exhaust emissions, obtained from the experimental tests.

The model considered in GT-Suite integrates in time the differential equations of motion for the vehicle and driveline components, resulting in the transient speeds and torque requested by the system. Data of indicated mean effective pressure (IMEP) are correlated to the engine speed and accelerator position and even as maps of emissions, air and fuel consumption, were used as input data from engine dynamometer experimental steady state conditions. Then, differential equations of vehicular motion were integrated in time, calculating transients of speed and torque and interpolating emissions and fuel consumption according to the load point demanded by the drive cycle condition. Equation 1 calculates the torque required for the vehicle motion, where the rolling resistance was calculated by the model as a function of drag coefficient, rolling friction and road grade.

$$\tau_{vehicle} = \left[I_{trans1} + \frac{I_{trans2}}{R_t^2} + \frac{I_{dsh}}{R_t^2} + \frac{I_{axl}}{(R_d^2)(R_t^2)} + \frac{(M_{veh})(r_{whl}^2)}{(R_d^2)(R_t^2)}\right]\frac{d\omega_{drv}}{dt} - \left[\frac{I_{trans2}}{R_t^3} + \frac{I_{dsh}}{R_t^3} + \frac{I_{axl}}{(R_d^2)(R_t^3)} + \frac{(M_{veh})(r_{whl}^2)}{(R_d^2)(R_t^3)}\right]\omega_{drv}\frac{dR_t}{dt} + \left[\frac{F_{aer} + F_{rol} + F_{grd}}{R_d R_t}\right]r_{whl} \quad \textbf{(1)}$$

The first term of Equation 1 represents the torque required to accelerate the effective inertia, evaluated at the clutch of the entire drivetrain, where $I_{trans1}$ and $I_{trans2}$ present the inertia in the input and output of transmission system, respectively. Moment of inertia in the driveshaft and axle are also given by $I_{dsh}$ and $I_{axl}$, and are related with the number of axles and inertia of each wheel, adapted to the vehicle characteristics. $R_d$ and $R_t$ are terms of final drive and transmission ratio for each gear. Wheel radius ($r_{whl}$) and vehicle mass ($M_{veh}$) are also in the first term of the equation. All these terms are directly related to the vehicle speed ($\omega_{drv}$) at the instant of time (t). The second term of Equation 1 represents the load induced by a transient gear ratio, using the information of vehicle transmission references. The third term of the equation add external forces as aerodynamics ($F_{aer}$), rolling resistance ($F_{rol}$) and gravity ($F_{grd}$)[56].

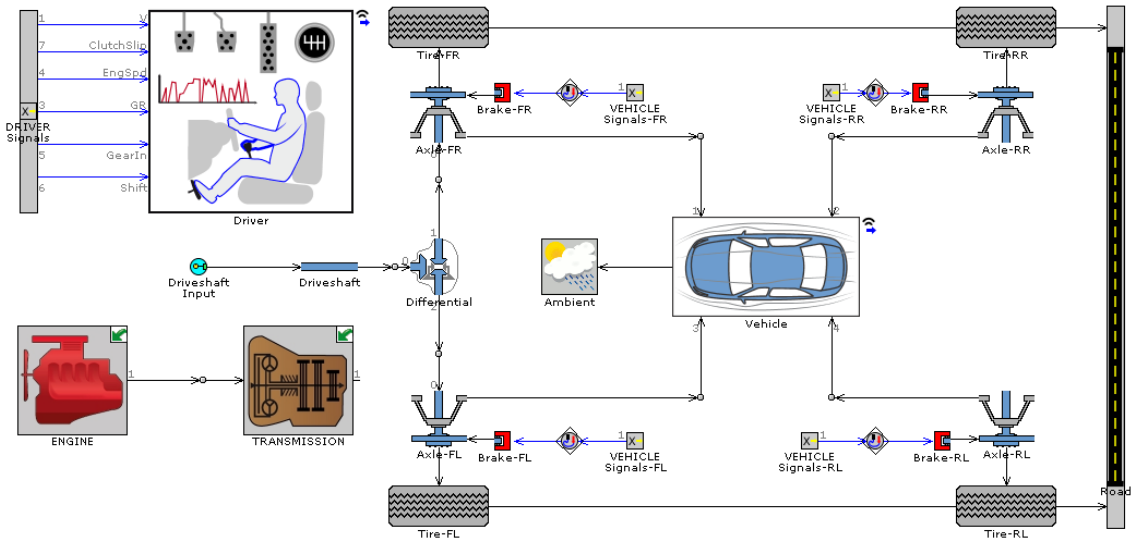


Figure 5. Vehicle model in GT-Suite software.

Table 5 presents input data considered for modelling as the driving cycles and the aerodynamics and gear ratios from a 2014 Ford Fiesta, which is the commercial vehicle originally equipped with the tested engine.

Table 5. Vehicle characteristics.

| **Vehicle** | |
|---|---|
| Tires size [mm/%/inch] | 185/60/15 |
| Vehicle mass [kg] | 1.29 |
| Passenger mass [kg] | 150 |
| Aerodynamic coefficient | 0.33 |
| Frontal area [m²] | 2.14 |
| Vehicle wheel base [m] | 2.489 |
| Axles | 2 |
| **Transmission** | |
| Gear ratio 1st [-] | 3.846 |
| Gear ratio 2st [-] | 2.038 |
| Gear ratio 3st [-] | 1.281 |
| Gear ratio 4st [-] | 0.951 |
| Gear ratio 5st [-] | 0.756 |
| Final drive ratio [-] | 4.56 |
| **Driving cycles** | |
| Standard | FTP-75 |
| | WLTC |
| Real | Free Flow |
| | Heavy Flow |

The computer model was also used to define the best strategy for the gear shifting, considering the different operation ranges presented in Figure 6. These ranges where established to cover conditions of maximum torque, maximum load and the extreme conditions obtained from the experimental tests. The gear shift strategy changes the permanence time in each region of the engine maps and is extremely important when optimizing exhaust emissions and fuel consumption.

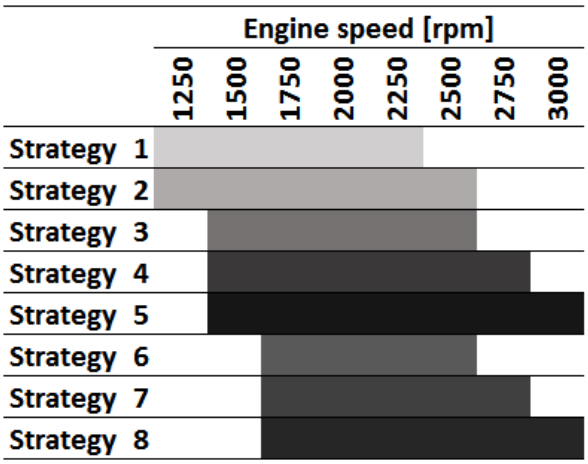


Figure 6. Eight gear shifting strategies evaluated for both computer models. The shadow regions present the engine speed range covered by each strategy.

## 3. Results and discussion

The results of this investigation are presented in two subsections. The first subsection presents the stationary engine maps in terms of exhaust emission and fuel consumption obtained through the experimental tests. With this, it is possible to observe the optimal operating regions for both ignition systems. The second subsection shows the specific emissions and fuel consumption according to the operating points in the engine maps, considering the baseline and the prechamber ignition systems in different driving conditions. For this, the best conditions of gear shift are evaluated to frame the engine operation in regions that improve the performance over the driving cycle. Cumulative exhaust emissions and fuel consumption for all conditions observed are also presented in this subsection.

### 3.1. Engine performance and exhaust emissions

Figure 7 presents the torque and power of the engine under wide open throttle conditions for the tested engine speed range. Although the maximum torque and power were probably not reached, the engine speeds were limited in order to represent what is observed in usual vehicular driving conditions, preserving the integrity of the engine. The reduction in the amount of fuel provided to the engine to operate with PCIS (λ=1.4) if compared to the baseline system (λ=1.0) also reduces in similar percentages the engine torque and power. However, the reduction in the combustion temperature and in the flame propagation speed with the use of lean mixtures can be helpful to mitigate knock occurrence [57], making it possible to increase the volumetric compression ratio and to adopt other strategies of performance recovery such as supercharging [19]. Furthermore, prechambers provide greater ignition energy, which allows the burning of lean mixtures with low levels of $CoV_{IMEP}$.

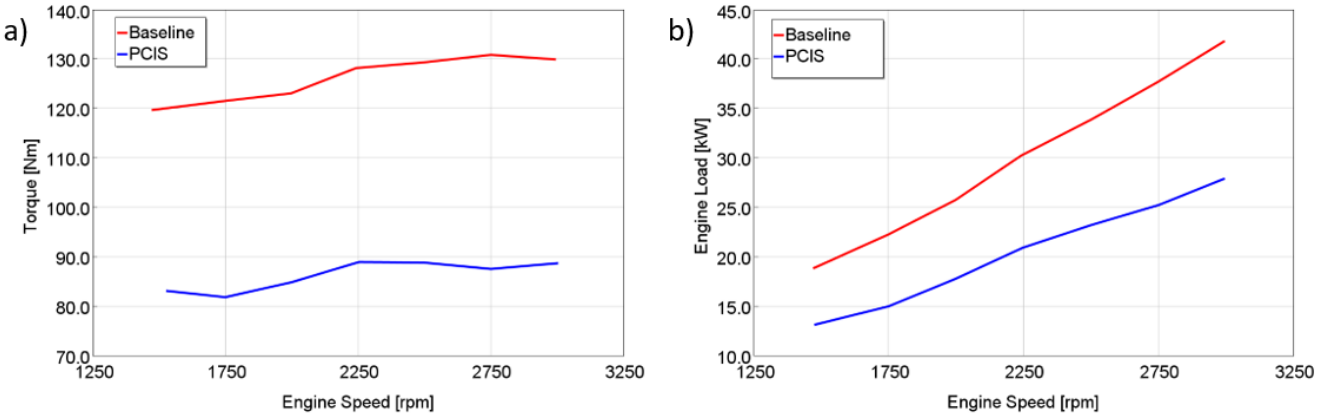


Figure 7. Maximum torque (a) and power (b) for the baseline ignition system and the PCIS, with λ=1.0 and λ=1.4 respectively, in different engine speeds.

The engine maps of fuel consumption and exhaust emissions (from the experimental points shown in Figure 2) are presented from Figure 8 to Figure 12. In all of them, specific values that extrapolate the scale, after the red regions in the maps, are not presented but are used in the simulation discussed in the following sections. Values presented for the engine speed of 3500 rpm are an extrapolation from the stationary points obtained up to 3000 rpm and are also necessary to the analysis performed in the following sections.

Figure 8 presents the specific fuel consumption for the baseline system (Figure 8a) and for the PCIS (Figure 8b). For the PCIS, the flow of hydrogen and ethanol were considered to determine the total specific fuel consumption. In low and medium engine speeds, the specific fuel consumption is not significantly altered with the use of PCIS. However, from 2000 rpm to 3000 rpm, in all load ranges, the reduction in specific fuel consumption is around 10% with respect to the conventional spark ignition system. This behaviour in the BSFC with the use of PCIS can be

justified by the lower pumping losses with the lean combustion, resultant from the need to increase the throttle opening to compensate the performance losses [46] and also by the reduction of combustion temperature, which reduces heat transfer losses. The benefits of the open valve are more observed under higher flow conditions, as in higher engine speeds and loads. This reduction of pumping losses in a spark-ignition engine at part load conditions is a challenge for improving the engine fuel economy, being subject of research in recent years, even more that these conditions are representative of urban driving cycles.

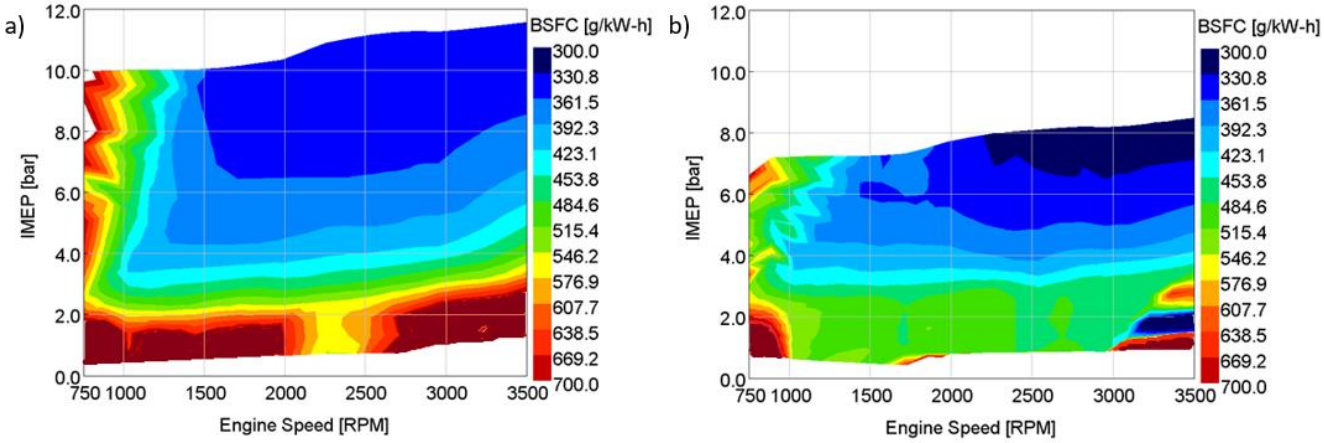


Figure 8. Specific fuel consumption for the engine with baseline (a) and pre-chamber (b) ignition system.

Besides the benefits on specific fuel consumption, one of the major goals of use lean mixtures is to reduce exhaust emissions such as NOx, which is one of the most expensive emissions to be reduced. Comparing the PCIS versus the baseline ignition system at Figure 9, it is seen that the most part of the engine map presents reductions between 80% to 90% in specific NOx emissions, with better values in part engine speeds and high loads. The lowest reduction was observed at low loads and part engine speeds, close to 2 bar of IMEP and between 1500 rpm and 2500 rpm, even though it was of the order of 70%. With this, a potential reduction in NOx exhaust emission can be expected in all of the possible engine applications, whether vehicular or in power generation, for example.

Due to the turbulence generated by the system and consequent homogenization of the mixture in the main chamber, the use of the prechamber ignition systems promote faster combustion than the baseline system if compared at the same air-fuel ratio. Then, the NOx formation, which depends of the presence of air, intake temperatures and time available for reactions between $N_2$ and $O_2$ to occur, will be less prone in faster combustions [14, 58]. In the conditions considered in this paper, the use of PCIS compensates the reduction in the combustion duration observed with the use of lean mixtures, reducing the time available for $N_2$ and $O_2$ reactions. Nevertheless, the joint use of PCIS and lean combustion strategies reduces the NOx thermal production in function of the lower temperatures involved in the combustion process [46].

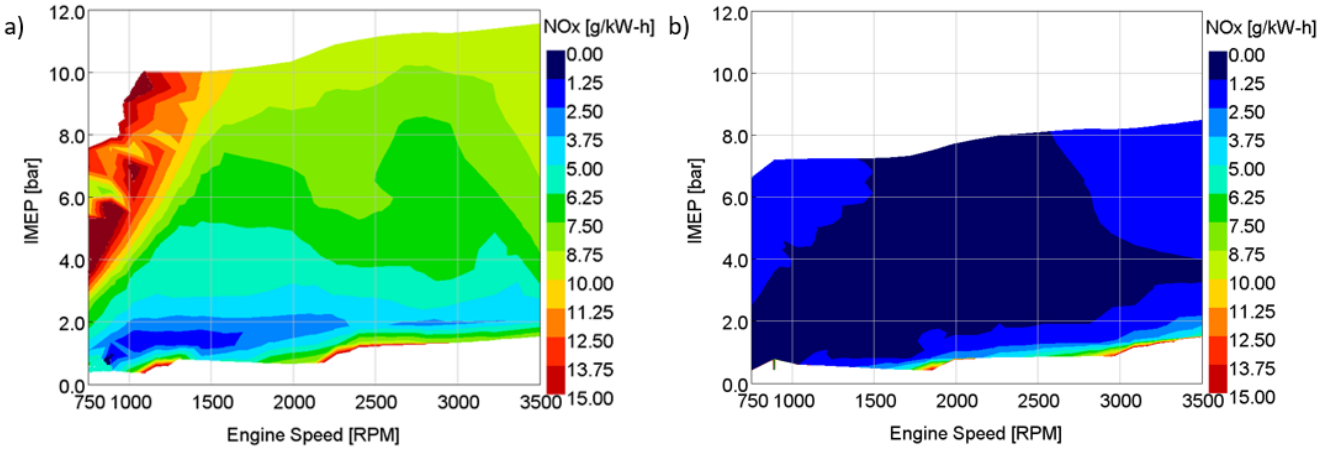


Figure 9. Specific $NO_X$ emission for the engine with baseline (a) and pre-chamber (b) ignition system.

Figure 10 show the maps of specific HC emission for both ignition systems. Either lean combustion strategy or the use of pre-chamber ignition system contribute to increase HC emissions. In lean combustion, the HC emissions rise due to increase of the quenching layer [59], since the combustion temperature is reduced as the mixture becomes leaner and the combustion threatens quench in the near-wall area, preventing the fuel from being fully converted and resulting in high losses. Although the PCIS presents a higher energy source than the traditional spark plug, being consequently able to promote the burning of lean mixtures, the increased turbulence generated by the prechamber also directs a larger amount of fuel to the crevices between the piston and the cylinder or between the valves and the cylinder head, being emitted as unburned hydrocarbons. Conditions of high loads and low engine speeds, around 6 to 7 bar of IMEP and up to 1500 rpm, presented the lowest increase in HC emissions with the use of PCIS and lean combustion, in the order of 20%. Worst results were observed for engine speeds higher than 1750 rpm, where the PCIS presented triple the specific HC emission of the conventional system.

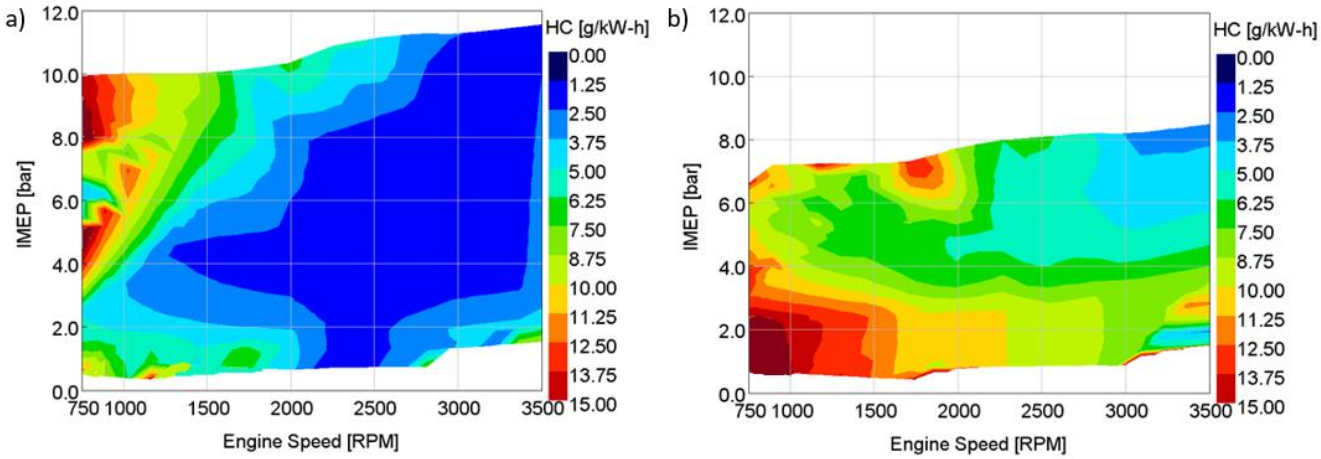


Figure 10. Specific HC emission for the engine with baseline (a) and pre-chamber (b) ignition system.

In baseline stoichiometric conditions, as presented in Figure 11a, the difficulty of generating a homogeneous air-fuel mixture results in incomplete combustion in some regions of the combustion chamber and consequently the formation of CO emissions. The excess of air in the PCIS concept due the operation with λ=1.4 results in a significant reduction in CO emissions, as observed in Figure 11b, when the oxidation of CO to $CO_2$ occurs. Especially with increasing load

and engine speed, the combustion chamber temperature and the turbulence levels rise, favoring a more complete combustion and, consequently, lower levels of CO specific emissions. CO emissions are reduced throughout the operating map by over than 60% with the use of PCIS, surpassing 75% from 2500 rpm and high loads.

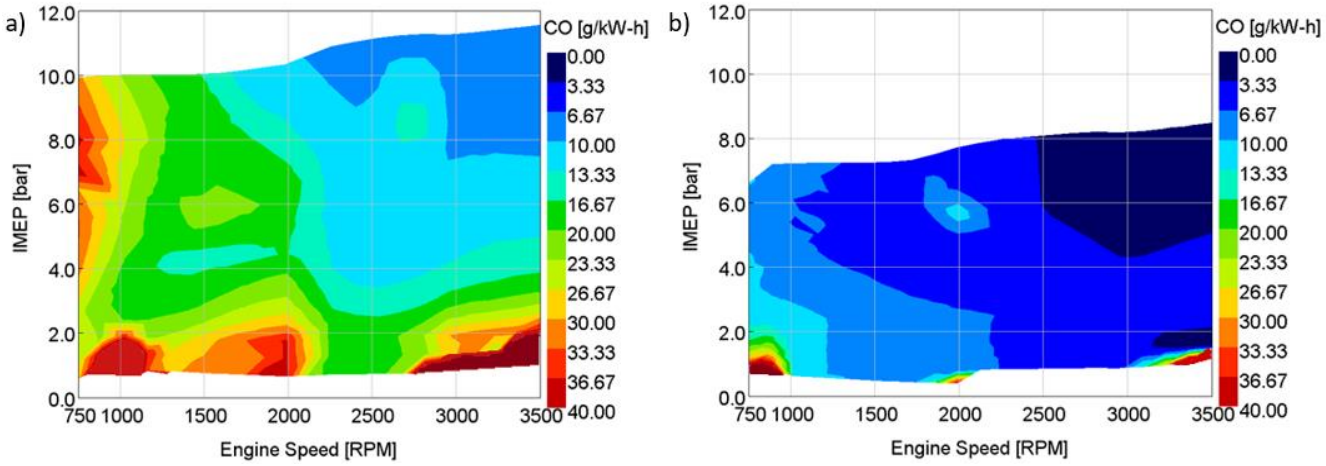


Figure 11. Specific CO emission for the engine with baseline (a) and pre-chamber (b) ignition system.

The complete hydrocarbon oxidation produces water and $CO_2$. Then, for conditions that provide a reduction in specific fuel consumption a reduction in $CO_2$ volumetric emission is also expected. At the same time, the reduction in specific fuel consumption resulting from a lean combustion does not necessarily reduces the specific $CO_2$ emission, since it is necessary to increase the air mass flow without significant reduction of fuel mass flow for the torque maintenance. This theory is verified in Figure 12, where the $CO_2$ emissions are very similar throughtout the engine map for both ignition systems, with maximum increases of 5% for the PCIS under conditions of high load and engine speeds, above of 2500 rpm and 6 bar of IMEP. In the other regions of the operating map, a reduction in $CO_2$ emissions between 5% and 10% is observed with the use of PCIS. The partial replacement of ethanol for hydrogen would lead to a reduction in $CO_2$ emissions, however, the need to conserve the mass causes rising in $CO_2$ and HC emissions especially in conditions where occurs significant reductions in CO emissions, as shown in Figures 10-12.

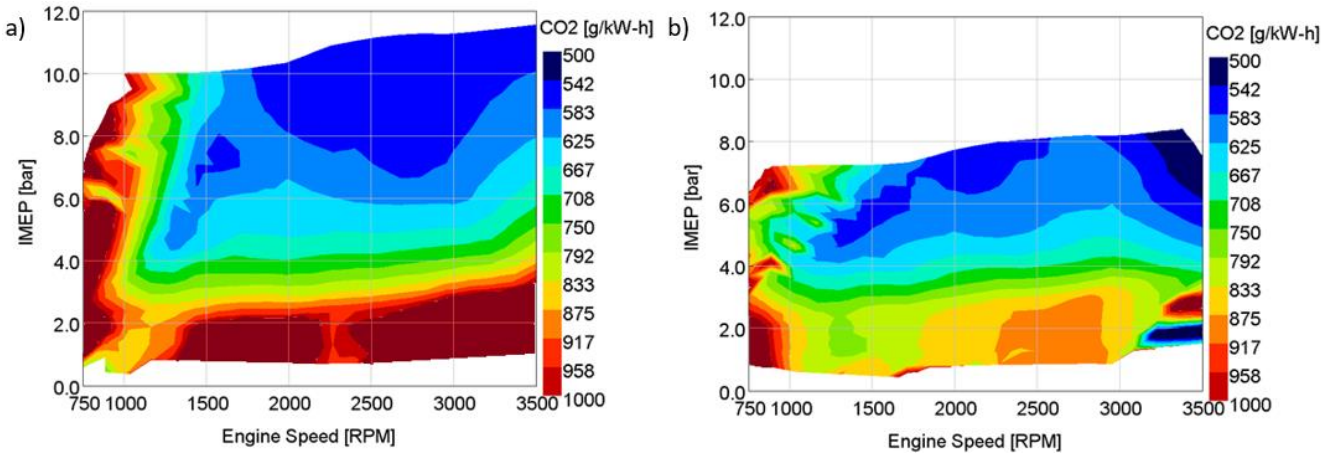


Figure 12. Specific $CO_2$ emission for the engine with baseline (a) and pre-chamber (b) ignition system.

### 3.2. Operation in driving cycles

This subsection is a combination of the experimental results obtained in stationary tests and the application of different driving conditions. To clarify the potential of the systems, it is essential to predict what will be observed when the systems are used in a vehicle. The computer model is able to simulate the vehicle with the baseline spark plug ignition system and with the PCIS covering the four different driving cycles. With this, operating points are generated through the experimental maps of fuel consumption and exhaust emissions, resulting in instantaneous and total values.

This subsection is divided into other two. The first one is intended to determine the better gear shift strategy that could provide the minor vehicle speed error for each ignition system when covering each driving cycle. With these results, the second item presents the optimal behaviour of the systems when applied to a vehicle in standard and real-world situations.

#### 3.2.1. Gear shift strategy

Eight gear shift strategies were evaluated using both ignition systems to cover the standard and real driving cycles. These ranges cover conditions of maximum torque, maximum load and the extreme conditions considered during stationary experimental tests. The main objective of this was to determine the strategy that would enable the vehicle to cover the driving cycles, even when operating with lean mixtures as considered to the PCIS. By this, different gear shift strategies are tested and the best was adopted in the simulation model aiming to present the results of the systems in their best operating conditions.

To evaluate the capability of each gear shift strategy, Table 6 presents the percentage reduction in the distance travelled relative to the total route of each driving cycle. According to these results, for all the cases, the gear shift strategy that made the vehicle better suited to the proposed cycle considered engine speeds of 1500 rpm to gear down-shifts and 3000 rpm to gear up-shifts.

Despite the performance losses presented in Figure 7, the vehicle model with PCIS was capable to cover the proposed driving cycle with all the gear shift strategies, presenting a maximum error of 6.28% in the WLTC distance to the optimized strategy. As also observed, the performance losses provide less impact in the real cycles if compared to the standardized cycles. Aiming at a more accurate comparison, the operation range between 1500 rpm and 3000 rpm was defined as the optimum condition in which the analysis of the driving cycles were carried out.

Table 6. Reduction of the distance travelled (%) with different strategies of gear shift, for both ignition systems in standard and real driving cycles.

| Operation Ranges | | Ignition System | Standard Cycles | | Real Cycles | |
|---|---|---|---|---|---|---|
| | | | FTP-75 | WLTC | Free Flow | Heavy Flow |
| **1250** | **2250** | **Baseline** | 9.96 | 5.26 | 3.49 | 3.69 |
| **1250** | **2500** | | 1.49 | 4.88 | 1.79 | 1.38 |
| **1500** | **2500** | | 3.84 | 4.74 | 4.53 | 4.20 |
| **1500** | **2750** | | 1.95 | 3.24 | 1.89 | 1.49 |
| **1500** | **3000** | | 0.95 | 2.73 | 1.39 | 1.11 |
| **1750** | **2500** | | 9.69 | 7.41 | 7.07 | 6.92 |
| **1750** | **2750** | | 5.72 | 4.24 | 4.93 | 4.27 |
| **1750** | **3000** | | 9.96 | 2.98 | 2.62 | 3.06 |
| **1250** | **2250** | **PCIS** | 9.67 | 12.48 | 7.59 | 7.39 |
| **1250** | **2500** | | 5.67 | 9.01 | 4.16 | 3.42 |
| **1500** | **2500** | | 9.22 | 14.79 | 7.00 | 8.23 |
| **1500** | **2750** | | 5.55 | 7.73 | 3.42 | 3.65 |
| **1500** | **3000** | | 3.34 | 6.28 | 2.44 | 1.91 |
| **1750** | **2500** | | 26.94 | 18.89 | 9.93 | 9.22 |
| **1750** | **2750** | | 9.92 | 12.32 | 6.84 | 7.45 |
| **1750** | **3000** | | 9.38 | 9.57 | 4.95 | 6.18 |

Figure 13 presents the simulated operation points of the engines when applied to the vehicle covering the standardized FTP-75 and WLTC with the optimized gear shift strategy. This Figure presents the extrapolated engine maps until 3500 rpm. As the WLTC is a mixed cycle, it also presents extra high speed conditions, as shown in Figure 6, which are only reached by the simulated vehicle in last gear and high engine speed. FTP-75 only presents urban conditions and therefore does not require accelerations above those defined for gear shifting. These various vehicle speed proposed by the WLTC cycle takes the engine to operate in a larger region of the map if compared to the FTP-75. By this, in cases of engine and systems optimizations, a larger region of the map should be considered when the vehicle is submitted to the WLTC.

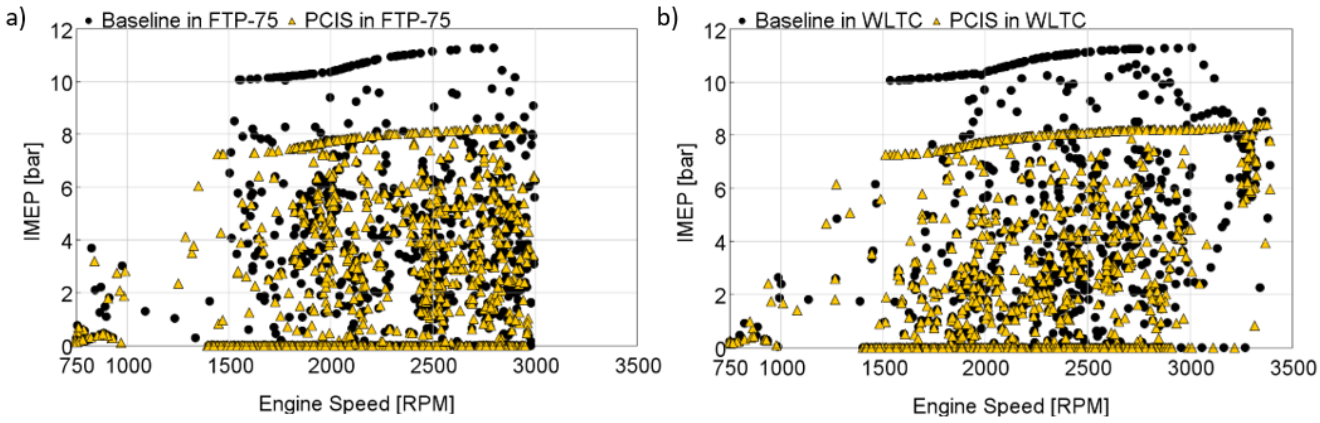


Figure 13. Operation points of the engine with both ignition systems for the optimized gear-shift strategy covering standardized FTP-75 (a) and WLTC (b) driving cycles.

Figure 14 shows the engine behaviour during the real urban driving cycles. In these conditions, all the operating points are contained within the range established by the gear shift except the high incidence under idle conditions, presented below 1000 rpm. As the performance parameters are impaired by the lean burn, more operation points in wide open throttle conditions are observed for PCIS.

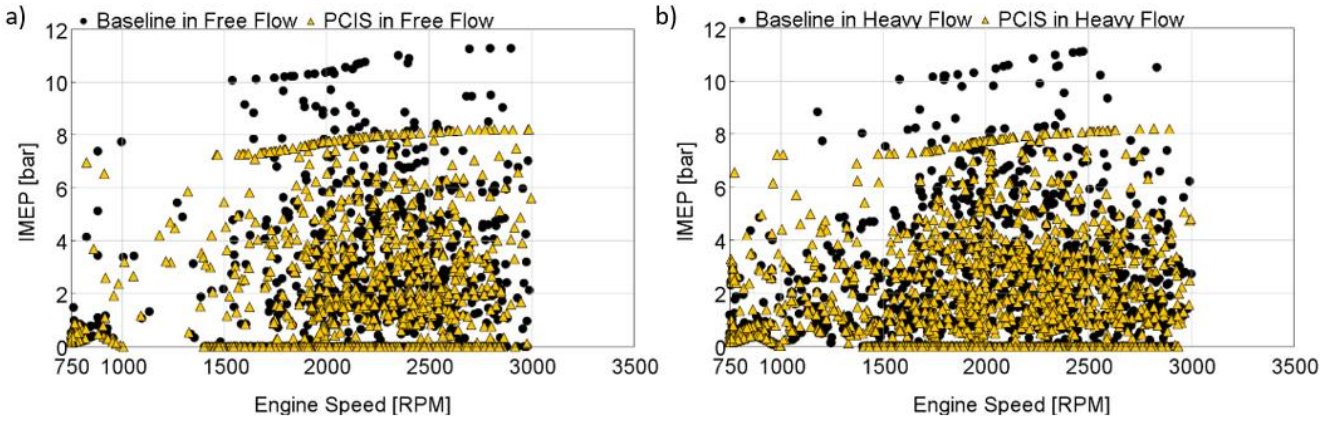


Figure 14. Operation points of the engine with both ignition systems for the optimized gear-shift strategy covering real world free flow (a) and heavy flow (b) driving cycles.

### 3.2.2. Fuel consumption and exhaust emissions

This subsection evaluates the potential of both ignition systems considering the operation in the range of better performance, as established in subsection 3.1, with regards in fuel consumption and engine-out emissions. Figure 15 to Figure 20 present the cumulative fuel consumption and exhaust emissions for the baseline system and for the PCIS through the standardized and real driving cycles. These results are estimated through the GT-Suite model previously described, considering the total duration of each driving cycle. In this analysis, the total fuel consumption is divided into ethanol and hydrogen, as shown in Figure 15 and Figure 16, respectively. Although the ethanol fuel consumption is lower for the engines with PCIS in the four analysed driving cycles, the hydrogen consumption that is not present in the baseline system must be considered for the purpose of operating costs. An expressive substitution of ethanol by hydrogen is observed under conditions of high engine speed and load, such as those corresponding to the extra high vehicle speed of the WLTC, where the engine operates above 2250 rpm. This is attributed to the need of hydrogen injection to reduce the $CoV_{IMEP}$ observed in this condition.

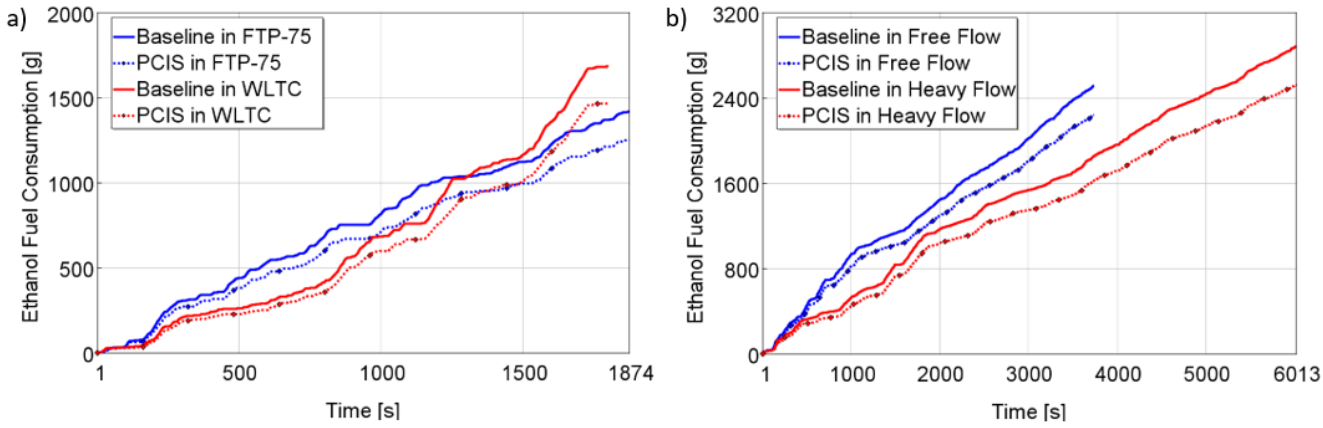


Figure 15. Ethanol consumed by the engine with both ignition systems for the optimized gear-shift strategy covering the standardized (a) and the real driving cycles (b).

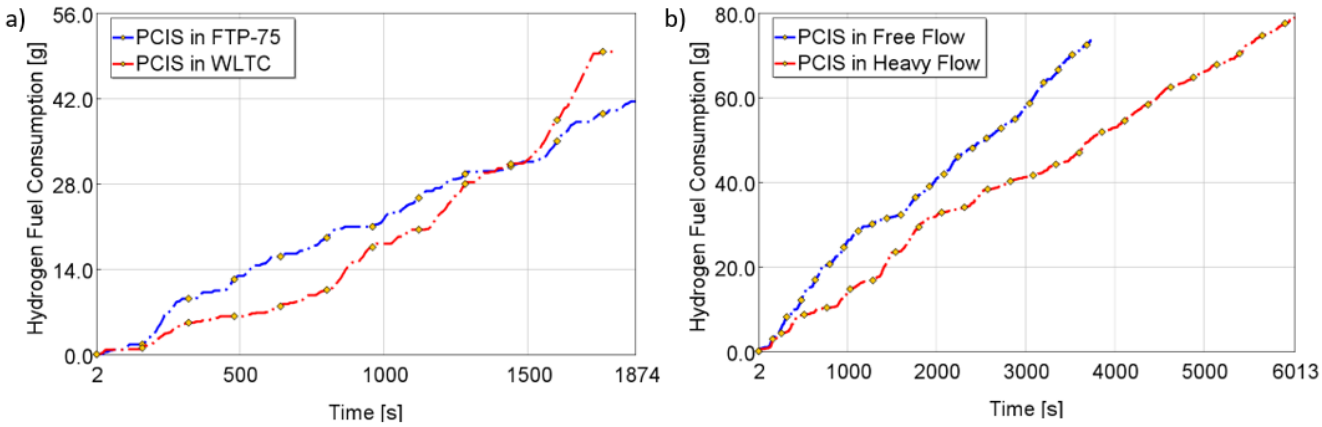


Figure 16. Hydrogen consumed by the engine with PCIS for the optimized gear-shift strategy covering the standardized (a) and the real driving cycles (b).

Figure 17 presents one of the major objectives of the prechamber uses to burning lean mixtures. The total NOx emission is similarly reduced in more than 80% for all the evaluated driving cycles when the PCIS is adopted. It is the result of the drastic reduction observed in all the NOx emission map. Regarding the driving characteristics, extra-high vehicle speeds, as observed in the WLTC, place the engine in conditions where higher NOx emissions occur, as observed through Figure 9 and Figure 13, pointing to higher specific NOx emissions under highway conditions with both ignition systems.

The incidence of idle conditions leads to increases in NOx emission rates as a function of the operation in low engine speeds and loads. However, despite the higher number of stops in real cycles if compared to standardized cycles, resulting in the lower vehicle average speeds presented in Table 4, the NOx emissions when in idle conditions are compensated with the engine load and speeds developed in acceleration conditions, representing an increase in the average positive acceleration also shown in Table 4.

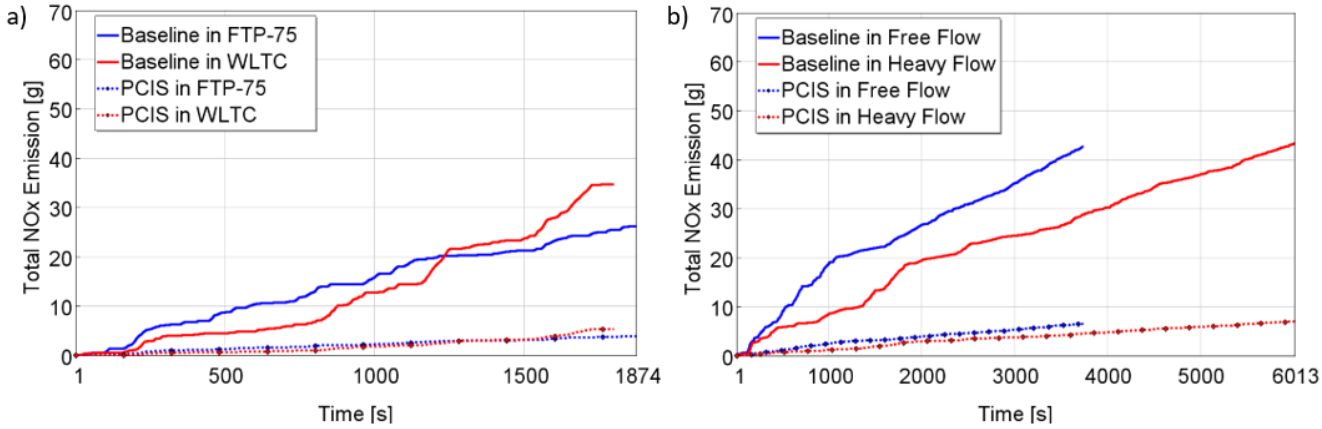


Figure 17. Total $NO_X$ emitted by the engine with both ignition systems for the optimized gear-shift strategy covering the standardized (a) and the real driving cycles (b).

According to the HC emission map, presented in Figure 10, better conditions could be observed in higher engine speeds, however, due to the stops in urban driving it is inevitable that the engine operate also at low conditions, providing the results of Figure 18. This tendency is also observed to CO and $CO_2$ emissions in Figure 19 and Figure 20. Optimization of the air-fuel mixture formation in the pre-chamber, of interconnecting holes arrangement and of spark plug

location can also be evaluated prior to the use of specific aftertreatment systems to control the hydrocarbon emissions.

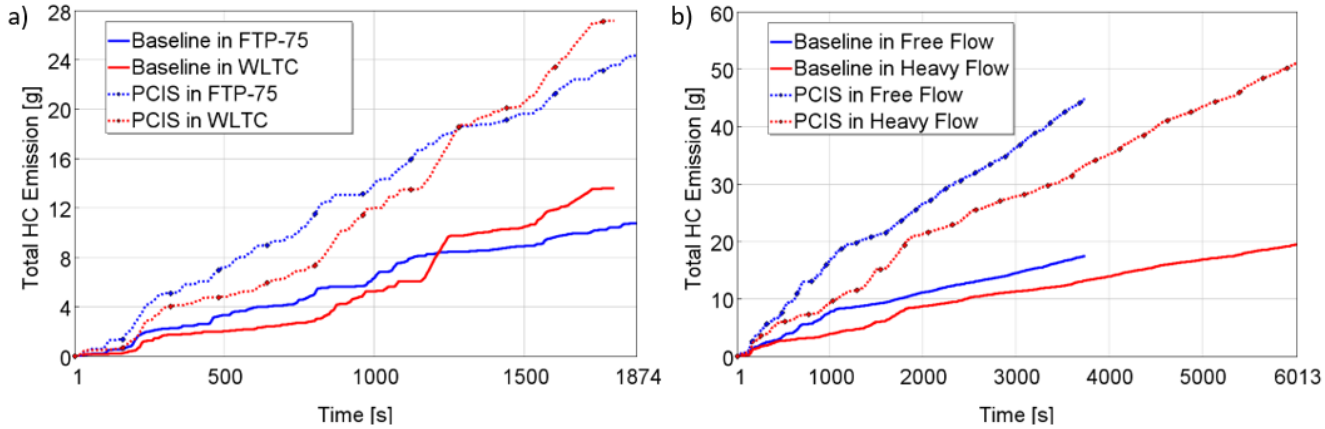


Figure 18. Total HC emitted by the engine with both ignition systems for the optimized gear-shift strategy covering the standardized (a) and the real driving cycles (b).

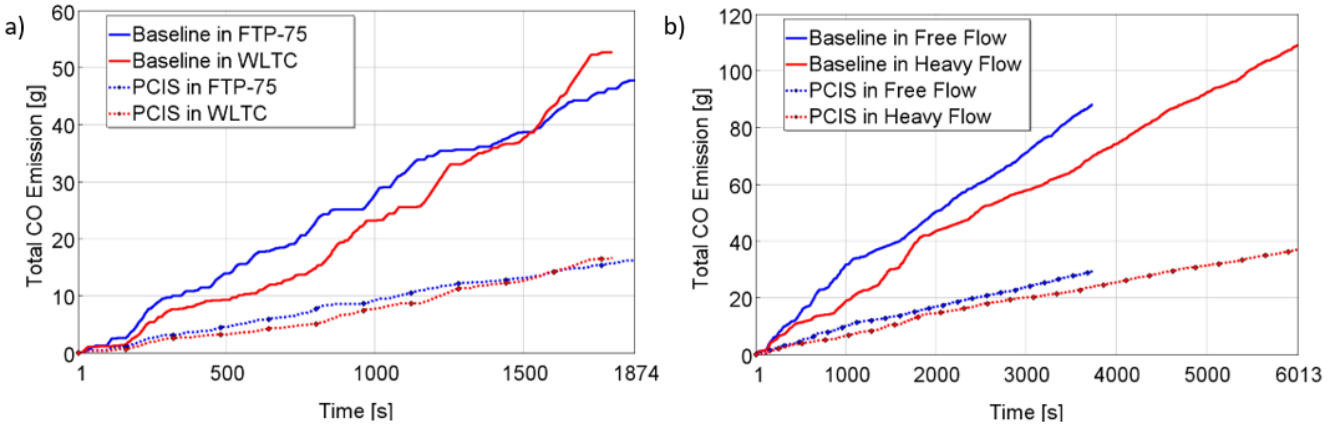


Figure 19. Total CO emitted by the engine with both ignition systems for the optimized gear-shift strategy covering the standardized (a) and the real driving cycles (b).

Higher emissions rate of CO and $CO_2$ are observed at the beginning of free flow real cycle compared to the heavy flow real cycle, in Figure 19b and Figure 20b, being generated due to the higher vehicle speeds developed in the initial 1000 seconds, as observed in Figure 4. Gear shift strategies for lower fuel consumption also place the engine with both ignition systems in the conditions of lower $CO_2$ exhaust emission. Despite of this, Figure 20 shows that the final $CO_2$ emission in driving cycles is almost the same, varying less than 2% when using the conventional spark plug or the prechamber ignition system.

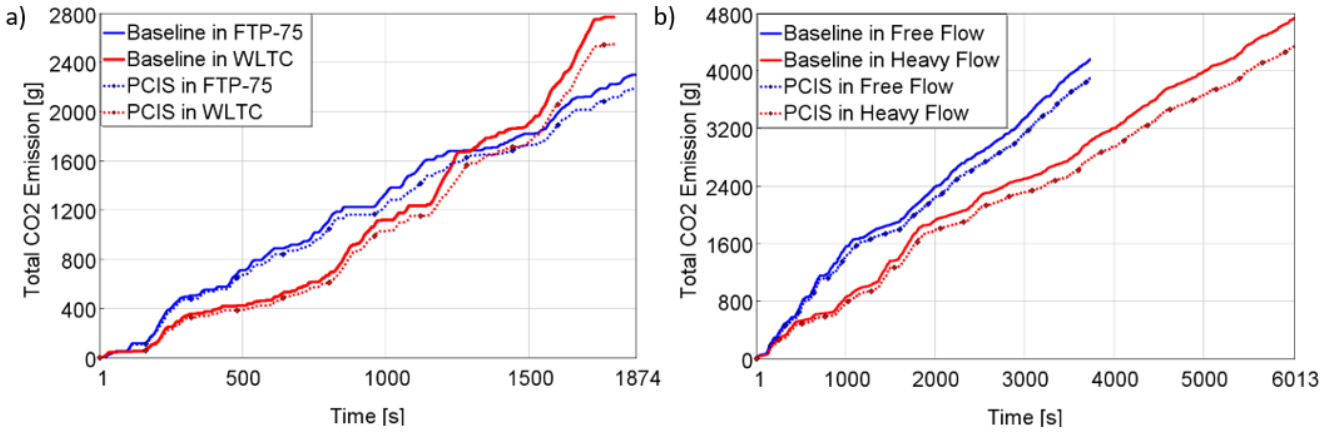


Figure 20. Total $CO_2$ emitted by the engine with both ignition systems for the optimized gear-shift strategy covering the standardized (a) and the real driving cycles (b).

Finally, Table 7 summarizes the average fuel consumption and raw exhaust emissions for the ignition systems when applied to a vehicle covering the different driving cycles. The biggest advantages of PCIS application is observed in the expressive reduction of $NO_x$ and CO emissions with minor influences over fuel consumption and $CO_2$ emissions. However, a solution must be so far provided to reduce HC emissions if the system were to be implemented in commercial applications.

Table 7. Exhaust emissions and fuel consumption comparison between the different driving cycles.

| | | FTP-75 | | WLTC | | Free Flow | | Heavy Flow | |
|---|---|---|---|---|---|---|---|---|---|
| | | **Baseline** | **PCIS** | **Baseline** | **PCIS** | **Baseline** | **PCIS** | **Baseline** | **PCIS** |
| **Ethanol Consumption** | **[g/km]** | 80.35 | 72.68 | 74.68 | 67.39 | 71.90 | 64.85 | 81.97 | 72.59 |
| **Hydrogen Consumption** | **[g/km]** | - | 2.42 | - | 2.29 | - | 2.13 | - | 2.27 |
| **NOx emissions** | **[g/km]** | 1.48 | 0.23 | 1.54 | 0.25 | 1.21 | 0.19 | 1.21 | 0.20 |
| **HC emissions** | **[g/km]** | 0.61 | 1.41 | 0.60 | 1.25 | 0.50 | 1.30 | 0.55 | 1.47 |
| **CO emissions** | **[g/km]** | 2.71 | 0.94 | 2.34 | 0.76 | 2.52 | 0.85 | 3.11 | 1.07 |
| **CO2 emissions** | **[g/km]** | 130.59 | 127.21 | 123.04 | 117.24 | 119.26 | 112.84 | 134.97 | 124.92 |

## 4. Conclusions

The present work has evaluated the lean burn potential of a prechamber ignition system by means of vehicle systems simulations. For this purpose, driving cycles representing the homologation procedures, such as FTP-75 and WLTC, and real driving cycles representing a specific route in southern Brazil were considered.

The comparison between the constructive characteristics of the standard and the real driving cycles have pointed to the influence of vehicular traffic and their impacts in fuel consumption and exhaust emissions. The simulated engine operation points show that the driving cycles used for homologation cover a larger region of the engine operating map when compared to real application, especially the WLTC with an extra high speed portion.

Eight gear shift strategies were evaluated in terms of vehicle performance, being optimized to 1500-3000 rpm for all the driving conditions. With this, the cumulative emissions and fuel consumption along the driving cycles were compared for both ignition systems. From these results, it was found that:

- The evolution of accumulated emissions and fuel consumption for the WLTC and FTP-75 have similar behaviour, while real conditions of free flow present a higher evolution rate if compared to the heavy flow. These rates are directly related to the vehicle speed developed in the driving cycles.
- The tendency of reduction in fuel consumption and exhaust emissions observed in the engine maps with PCIS are confirmed when are covered the driving cycles.
- Despite the reduction in performance parameters with the lean burn, the vehicle was capable to cover the proposed routes with speed variations within the allowed by the vehicular test standards.

Finally, the summary of average engine-out emissions and performance results for all the driving cycles and ignition modes reveals that:

- The standard cycles considered in this study presented similar results to those observed for the real cycles, making them representative for the estimation of real-world emissions.
- Despite the hydrogen injection to control combustion stability, the average fuel consumption for the PCIS is at least 7% lower if compared to the baseline in all the driving cycles. The $CO_2$ emissions presented the same tendency of fuel consumption and remained lower for all the PCIS cases.
- The PCIS provided its potential to reduce $NO_x$ emissions, with values of more than 85% of reduction in all the considered cycles. Emissions of CO also were reduced in more than 65%.
- HC emissions presented a notable increment, especially in real-world conditions, indicating the need to evaluate possible improvements in the PCIS or the adoption of aftertreatment systems.

**References**


[1] A. Ramos, J. Muñoz, F. Andrés, and O. Armas, "NOx emissions from diesel light duty vehicle tested under NEDC and real-word driving conditions," *Transportation Research Part D: Transport and Environment,* vol. 63, pp. 37-48, 2018.

[2] *Comission Regulation (EU) 2016/427 of 10 March 2016 amending Regulation (EC) N°692/2008 as regards emissions from light passenger and commercial vehicles (Euro 6)*.

[3] I. B. D. M. A. E. D. R. N. RENOVÁVEIS, "Programa de controle da poluição do ar por veículos automotores-Proconve/Promot/Ibama," ed: Ibama/Diqua Brasília, 2011.

[4] I. P. O. C. Change, "IPCC," *Climate change,* 2014.

[5] O. de Salvo Junior and F. G. V. de Almeida, "Influence of technologies on energy efficiency results of official Brazilian tests of vehicle energy consumption," *Applied Energy,* vol. 241, pp. 98-112, 2019.

[6] H. K. Noh and S.-Y. No, "Effect of bioethanol on combustion and emissions in advanced CI engines: HCCI, PPC and GCI mode–A review," *Applied energy,* vol. 208, pp. 782-802, 2017.

[7] T. D. M. Lanzanova, M. Dalla Nora, and H. Zhao, "Performance and economic analysis of a direct injection spark ignition engine fueled with wet ethanol," *Applied energy,* vol. 169, pp. 230-239, 2016.

[8] M. M. Koupaie, A. Cairns, H. Vafamehr, and T. D. M. Lanzanova, "A study of hydrous ethanol combustion in an optical central direct injection spark ignition engine," *Applied Energy,* vol. 237, pp. 258-269, 2019.

[9] V. B. Pedrozo and H. Zhao, "Improvement in high load ethanol-diesel dual-fuel combustion by Miller cycle and charge air cooling," *Applied energy,* vol. 210, pp. 138-151, 2018.

[10] R. B. R. da Costa *et al.*, "Combustion, performance and emission analysis of a natural gas-hydrous ethanol dual-fuel spark ignition engine with internal exhaust gas recirculation," *Energy Conversion and Management,* vol. 195, pp. 1187-1198, 2019.

[11] J. Benajes, A. García, J. Monsalve-Serrano, and V. Boronat, "Dual-fuel combustion for future clean and efficient compression ignition engines," *Applied Sciences,* vol. 7, no. 1, p. 36, 2016.

[12] J. Kim, K. M. Chun, S. Song, H.-K. Baek, and S. W. Lee, "Hydrogen effects on the combustion stability, performance and emissions of a turbo gasoline direct injection engine in various air/fuel ratios," *Applied energy,* vol. 228, pp. 1353-1361, 2018.

[13] S. B. Shrestha and G. Karim, "Hydrogen as an additive to methane for spark ignition engine applications," *International Journal of Hydrogen Energy,* vol. 24, no. 6, pp. 577-586, 1999.

[14] A. Ramadhas, P. K. Singh, P. Sakthivel, R. Mathai, and A. K. Sehgal, "Effect of ethanol-gasoline blends on combustion and emissions of a passenger car engine at part load operations," SAE Technical Paper, 0148-7191, 2016.

[15] T. Pachiannan, W. Zhong, S. Rajkumar, Z. He, X. Leng, and Q. Wang, "A literature review of fuel effects on performance and emission characteristics of low-temperature combustion strategies," *Applied Energy,* vol. 251, p. 113380, 2019.

[16] C. E. C. Alvarez, V. R. Roso, G. E. Couto, and R. M. Valle, "Combustion Analysis of a Current Vehicular Engine Operating in Lean Air-Fuel Conditions," SAE Technical Paper, 0148-7191, 2017.

[17] C. E. C. Alvarez, G. E. Couto, V. R. Roso, A. B. Thiriet, and R. M. Valle, "A review of prechamber ignition systems as lean combustion technology for SI engines," *Applied Thermal Engineering,* vol. 128, pp. 107-120, 2018.

[18] C. E. C. Alvarez, G. E. Couto, V. R. Roso, A. B. Thiriet, and R. M. Valle, "A review of Prechamber Ignition Systems as Lean Combustion Technology for SI Engines," *Applied Thermal Engineering,* 2017.

[19] J. Benajes, R. Novella, J. Gomez-Soriano, P. Martinez-Hernandiz, C. Libert, and M. Dabiri, "Evaluation of the passive pre-chamber ignition concept for future high compression ratio turbocharged spark-ignition engines," *Applied Energy,* vol. 248, pp. 576-588, 2019.

[20] T. Date, S. Yagi, A. Ishizuya, and I. Fujii, "Research and development of the Honda CVCC engine," SAE Technical Paper, 0148-7191, 1974.

[21] A. Scussel, A. Simko, and W. Wade, "The Ford PROCO engine update," SAE Technical Paper, 0148-7191, 1978.

[22] W. R. Brandstetter, G. Decker, and K. Reichel, "The Water-Cooled Volkswagen PCI-Stratified Charge Engine," SAE Technical Paper, 0148-7191, 1975.

[23] W. R. Brandstetter, G. Decker, H. Schafer, and D. Steinke, "The Volkswagen PCI Stratified Charge Concept-Results from the 1.6 Liter Air Cooled Engine," SAE Technical Paper, 0148-7191, 1974.

[24] D. Gruden, "Combustion and Exhaust Emission of an Engine Using the Porsche-Stratified-Charge-Chamber-System," SAE Technical Paper, 0148-7191, 1975.

[25] M. Noguchi, S. Sanda, and N. Nakamura, "Development of Toyota lean burn engine," SAE Technical Paper, 0148-7191, 1976.

[26] W. P. Attard, M. Bassett, P. Parsons, and H. Blaxill, "A new combustion system achieving high drive cycle fuel economy improvements in a modern vehicle powertrain," SAE Technical Paper, 0148-7191, 2011.

[27] G. Fontaras, N.-G. Zacharof, and B. Ciuffo, "Fuel consumption and CO2 emissions from passenger cars in Europe–Laboratory versus real-world emissions," *Progress in Energy and Combustion Science,* vol. 60, pp. 97-131, 2017.

[28] Z. Mera, N. Fonseca, J.-M. López, and J. Casanova, "Analysis of the high instantaneous NOx emissions from Euro 6 diesel passenger cars under real driving conditions," *Applied Energy,* vol. 242, pp. 1074-1089, 2019.

[29] P. Iodice and A. Senatore, "Experimental-analytical investigation to estimate an emission inventory from road transport sector," in *IAENG Transactions on Engineering Sciences—Special Issue of the International MultiConference of Engineers and Computer Scientists, IMECS 2013 and World Congress on Engineering, WCE*, 2014, vol. 2013, pp. 141-149.

[30] P. Iodice and A. Senatore, "Industrial and urban sources in Campania, Italy: The air pollution emission inventory," *Energy & Environment,* vol. 26, no. 8, pp. 1305-1317, 2015.

[31] T. Khan and H. C. Frey, "Comparison of real-world and certification emission rates for light duty gasoline vehicles," *Science of The Total Environment,* vol. 622, pp. 790-800, 2018.

[32] R. Oldenkamp, R. van Zelm, and M. A. Huijbregts, "Valuing the human health damage caused by the fraud of Volkswagen," *Environmental pollution,* vol. 212, pp. 121-127, 2016.

[33] (2017). *Real-Driving Emissions Test Procedure for Exhaust Gas Pollutant Emissions of Cars and Light Commercial Vehicles in Europe*.

[34] G. Fontaras, V. Franco, P. Dilara, G. Martini, and U. Manfredi, "Development and review of Euro 5 passenger car emission factors based on experimental results over various driving cycles," *Science of the Total Environment,* vol. 468, pp. 1034-1042, 2014.

[35] J. M. Luján, V. Bermúdez, V. Dolz, and J. Monsalve-Serrano, "An assessment of the real-world driving gaseous emissions from a Euro 6 light-duty diesel vehicle using a portable emissions measurement system (PEMS)," *Atmospheric environment,* vol. 174, pp. 112-121, 2018.

[36] A. García, J. Monsalve-Serrano, V. R. Roso, and M. E. S. Martins, "Evaluating the emissions and performance of two dual-mode RCCI combustion strategies under the World Harmonized Vehicle Cycle (WHVC)," *Energy Conversion and Management,* vol. 149, pp. 263-274, 2017.

[37] A. García, J. Monsalve-Serrano, R. Sari, N. Dimitrakopoulos, M. Tunér, and P. Tunestål, "Performance and emissions of a series hybrid vehicle powered by a gasoline partially premixed combustion engine," *Applied Thermal Engineering,* vol. 150, pp. 564-575, 2019.

[38] J. Benajes, A. García, J. Monsalve-Serrano, and S. Martínez-Boggio, "Optimization of the parallel and mild hybrid vehicle platforms operating under conventional and advanced combustion modes," *Energy Conversion and Management,* vol. 190, pp. 73-90, 2019.

[39] J. Benajes, A. García, J. Monsalve-Serrano, and R. L. Sari, "Fuel consumption and engine-out emissions estimations of a light-duty engine running in dual-mode RCCI/CDC with different fuels and driving cycles," *Energy,* vol. 157, pp. 19-30, 2018.

[40] A. García, P. Piqueras, J. Monsalve-Serrano, and R. L. Sari, "Sizing a conventional diesel oxidation catalyst to be used for RCCI combustion under real driving conditions," *Applied Thermal Engineering,* vol. 140, pp. 62-72, 2018.

[41] N. D. S. A. Santos, C. E. C. Alvarez, V. R. Roso, J. G. C. Baeta, and R. M. Valle, "Combustion analysis of a SI engine with stratified and homogeneous pre-chamber ignition system using ethanol and hydrogen," *Applied Thermal Engineering,* p. 113985, 2019.

[42] F. A. Rodrigues Filho, G. E. Couto, R. M. Valle, V. R. Roso, and C. C. Alvarez, "Sistema de ignição com pré-câmara de mistura estratificada para motores de combustão interna " Brasil, 2018.
[43] (2015). *RESOLUÇÃO ANP Nº 19, DE 15.4.2015 - DOU 16.4.2015 - Regulamenta a composição, comercialização e coloração do etanol".*
[44] (2015). *PORTARIA Nº - 75, DE 5 DE MARÇO DE 2015, Percentual obrigatório de adição de etanol anidro combustível à gasolina.*
[45] T. Melo, "Análise experimental e simulação computacional de um motor flex operando com diferentes misturas de etanol hidratado na gasolina," *Rio de Janeiro. Tese de Doutorado. COPPE, Universidade Federal do Rio de Janeiro,* 2012.
[46] V. R. Roso, N. D. S. A. Santos, C. E. C. Alvarez, F. A. Rodrigues Filho, F. J. P. Pujatti, and R. M. Valle, "Effects of mixture enleanment in combustion and emission parameters using a flex-fuel engine with ethanol and gasoline," *Applied Thermal Engineering,* 2019.
[47] A. Mariani, F. Foucher, and B. Moreau, "The effects of a radio frequency ignition system on the efficiency and the exhaust emissions of a spark-ignition engine," SAE Technical Paper, 0148-7191, 2013.
[48] V. R. Roso and M. E. S. Martins, "Simulation of Fuel Consumption and Emissions for Passenger Cars and Urban Buses in Real-World Driving Cycles," SAE Technical Paper, 0148-7191, 2016.
[49] V. R. Roso and M. E. S. Martins, "Evaluation of a Real-World Driving Cycle and its impacts on fuel consumption and emissions," SAE Technical Paper, 0148-7191, 2015.
[50] (2014). ***Global Technical Regulation No. 15 (Worldwide harmonized Light vehicles Test Procedure)***.
[51] J. D. Bishop, N. Molden, and A. M. Boies, "Using portable emissions measurement systems (PEMS) to derive more accurate estimates of fuel use and nitrogen oxides emissions from modern Euro 6 passenger cars under real-world driving conditions," *Applied Energy,* vol. 242, pp. 942-973, 2019.
[52] T. J. BARLOW, S. Latham, I. McCrae, and P. Boulter, "A reference book of driving cycles for use in the measurement of road vehicle emissions," *TRL Published Project Report,* 2009.
[53] J. Kent, G. Allen, and G. Rule, "A driving cycle for Sydney," *Transportation Research,* vol. 12, no. 3, pp. 147-152, 1978.
[54] S. K. Pathak, V. Sood, Y. Singh, and S. Channiwala, "Real world vehicle emissions: Their correlation with driving parameters," *Transportation Research Part D: Transport and Environment,* vol. 44, pp. 157-176, 2016.
[55] C. J. T. van de Weijer, *Heavy-Duty Emission Factors: Development of representative driving cycles and prediction of emissions in real-life*. na, 1997.
[56] G. Technologies, "GT- Suite: Engine Performance Application Manual 7.6," 2016.
[57] X. Duan *et al.*, "Performance, combustion and knock assessment of a high compression ratio and lean-burn heavy-duty spark-ignition engine fuelled with n-butane and liquefied methane gas blend," *Energy,* vol. 158, pp. 256-268, 2018.
[58] K. Varatharajan and M. Cheralathan, "Influence of fuel properties and composition on NOx emissions from biodiesel powered diesel engines: A review," *Renewable and sustainable energy reviews,* vol. 16, no. 6, pp. 3702-3710, 2012.
[59] D. Dunn-Rankin, *Lean combustion: technology and control*. Academic Press, 2011.

**Acknowledgments**

The authors would like to thank the Post-Graduation Program in Mechanical Engineering at

UFMG, the CTM – Centro de Tecnologia da Mobilidade at UFMG, the CMT – Motores Térmicos at UPV and research supporting agencies by CAPES and FAPEMIG for the support provided.

**Definitions/Abbreviations**

| | |
|---|---|
| E96 | Brazilian Commercial Hydrous Ethanol |
| $CO_2$ | Carbon Dioxide |
| CO | Carbon Monoxide |
| CLD | Chemiluminescente detection |
| CoV | Coefficient of Variation |
| CA | Crankangle |
| ECU | Electronic Central Unit |
| FTP-75 | Federal Test Procedure |
| FID | Flame Ionization Detector |
| HC | Hydrocarbon |
| $H_2O$ | Water |
| IMEP | Indicated Effective Mean Pressure |
| IPCC | International Panel of Climate Changes |
| ISFC | Indicated Specific Fuel Consumption |
| LHV | Lower Heating Value |
| MC | Main Chamber |
| MBF | Mass Burned Fraction |
| MBT | Maximum Brake Torque |
| NEDC | New European Driving Cycle |
| $NO_x$ | Nitrogen Oxides |
| OBD | On Board Diagnostic |
| OBS | On-Board System |
| $O_2$ | Oxygen |
| PFI | Port Fuel injection |
| PKE | Positive Kinetic Energy |
| PC | Pre-Chamber |
| PCIS | Pre-Chamber Ignition System |
| SI | Spark Ignition |

| | |
|---|---|
| RPA | Relative Positive Acceleration |
| RMS | Root Mean Square |
| TWC | Three-Way Catalytic Converter |
| THC | Total Hydrocarbon |
| WOT | Wide Open Throttle |
| WLTC | Worldwide harmonized Light vehicles Test Cycles |